

DOI: 10.1002/chem.201303026

Fluorescence Modulation in Tribranched Switchable [4]Rotaxanes

Ji-Na Zhang, Hong Li, Wei Zhou, Shi-Lin Yu, Da-Hui Qu,* and He Tian^[a]

Abstract: Two novel tribranched [4]rotaxanes with a 1,3,5-triphenylene core and three rotaxane arms have been designed, synthesized, and characterized by ¹H and ¹³C NMR spectroscopies and HR-ESI mass spectrometry. [4]Rotaxanes **1** and **2** each possess the same three-armed skeleton. Each arm incorporates two distinguishable binding sites for a dibenzo[24]crown-8 ring, namely a dibenzylammonium site and an *N*-methyltriazolium site, and is terminated by a 4-morpholino-naphthalimide fluorophore as a stopper. [4]Rotaxane **1** has three di-ferrocene-functionalized dibenzo[24]crown-8 rings whereas **2** has three simple dibenzo[24]crown-8 rings interlocked

with the thread component. Uniform shuttling motions of the three macrocycles in both **1** and **2** can be driven by external acid–base stimuli, which were confirmed by ¹H NMR spectroscopy. However, [4]rotaxanes **1** and **2** show distinct modes of fluorescence modulation in response to external acid–base stimuli. [4]Rotaxane **1** exhibits a remarkable fluorescence decrease in response to the addition of 1,8-diazabicyclo[5.4.0]undec-7-ene (DBU)

as a base, which can displace the ferrocene-functionalized macrocycle from the dibenzylammonium station to the *N*-methyltriazolium station. In contrast, the fluorescence intensity of [4]rotaxane **2** showed an enhancement with the addition of DBU. Time-resolved fluorescence measurements have been performed. The different photoinduced electron-transfer processes responsible for the fluorescence changes in the two molecular systems are discussed. Topological structures of this kind have significant potential for the design and construction of large and complex assemblies with controllable functions.

Keywords: bistable rotaxanes · click chemistry · fluorescence · function · photoinduced electron transfer

Introduction

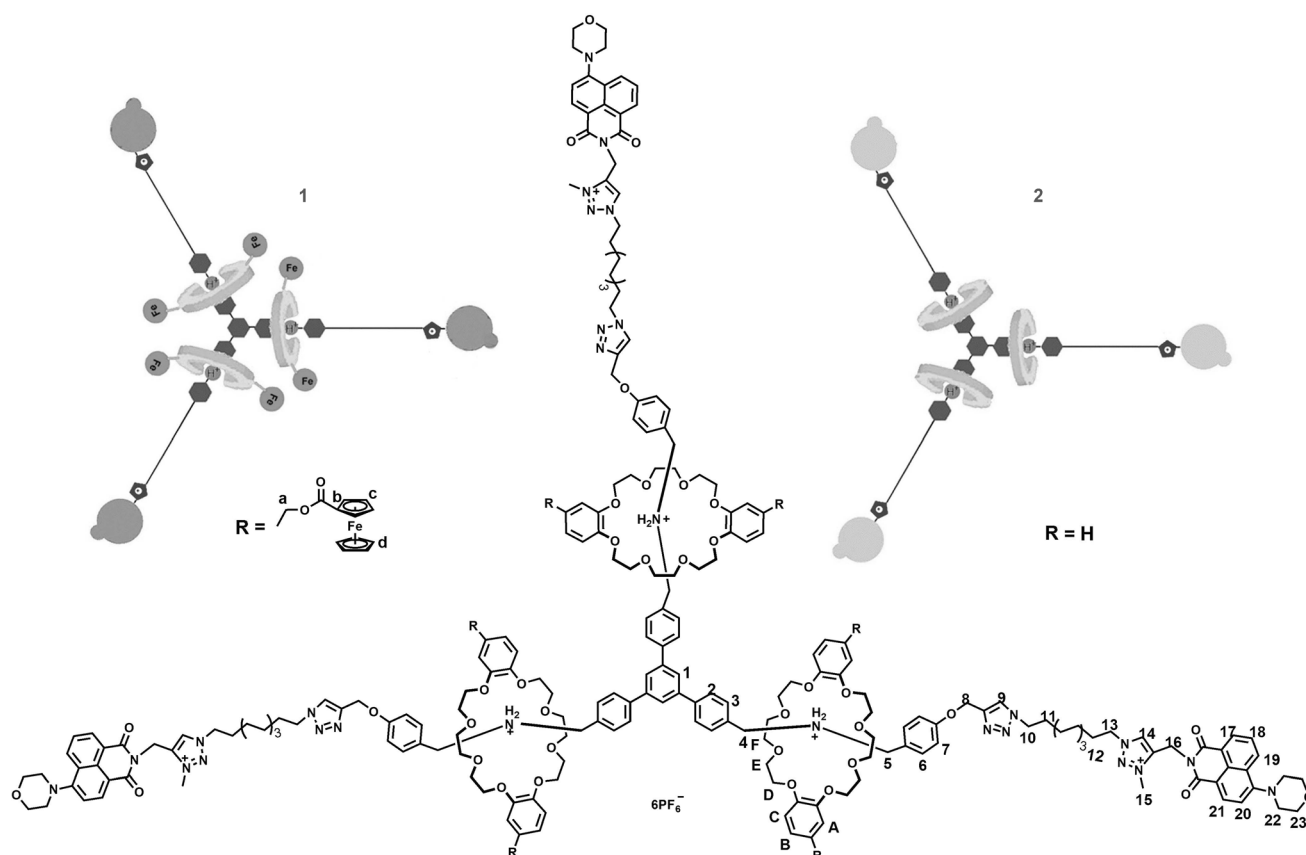
Mechanically interlocked molecules (MIMs) have attracted a great deal of attention because of their applications in molecular devices and as components of molecular machinery.^[1–3] Bistable [2]rotaxanes, in which a macrocycle is interlocked with a dumbbell-shaped component and can shuttle between two distinct, well-separated recognition sites on the thread component in response to external stimuli, have emerged as the most common types of MIMs because of their adjustable and controllable properties.^[4] However, the synthesis of highly ordered [*n*]rotaxane systems having multi-branched structures with repeating bistable [2]rotaxane units still remains a challenge because of their complex structures and difficult reaction steps.^[5] The introduction of molecular building blocks with specific shapes can lead to the formation of [*n*]rotaxanes with fixed configurations.^[5b,6] This fact inspired chemists to employ various symmetrical

molecular building blocks to construct highly symmetrical [*n*]rotaxane systems. On the other hand, it is desirable to develop more sophisticated mechanically interlocked molecules that combine complicated structures and increased functional complexity, by introducing functional units^[7] to achieve specific functions and to realize intercomponent interactions such as electron transfer,^[8] energy transfer,^[9] charge transfer,^[10] and so on. To date, much work has been focused on the design and construction of multifunctional bistable and multistable [2]rotaxanes, the distinct states of which can be recognized by various output signals, such as fluorescence,^[4a,e,11] electrochemical signals,^[7b,12] circular dichroism,^[13] and so on. Unlike for [2]rotaxane systems, of which there are already many fascinating examples,^[4] reports of highly ordered bistable [*n*]rotaxanes with a symmetrical core, especially reports that demonstrate uniform shuttling motion of several macrocycles and controllable photo-physical property changes in response to external stimuli, are very rare.^[5b]

Herein, we report the design, construction, and characterization of two novel functional symmetrical [4]rotaxanes having tribranched structures. As shown in Scheme 1, the two novel tribranched [4]rotaxanes **1** and **2** are based on a 1,3,5-triphenylene unit as the core, to which three rotaxane arms threaded through different macrocycles are covalently connected. [4]Rotaxanes **1** and **2** have the same three-armed skeleton, which incorporates two distinct stations for dibenzo[24]crown-8 (DB24C8) rings, namely a dibenzylam-

[a] J.-N. Zhang, H. Li, W. Zhou, S.-L. Yu, Dr. D.-H. Qu, Prof. Dr. H. Tian
Key Laboratory for Advanced Materials and Institute of Fine Chemicals
East China University of Science & Technology
Shanghai 200237 (P. R. China)
Fax: (+86) 21-64252288
E-mail: dahui_qu@ecust.edu.cn

Supporting information for this article is available on the WWW under <http://dx.doi.org/10.1002/chem.201303026>.



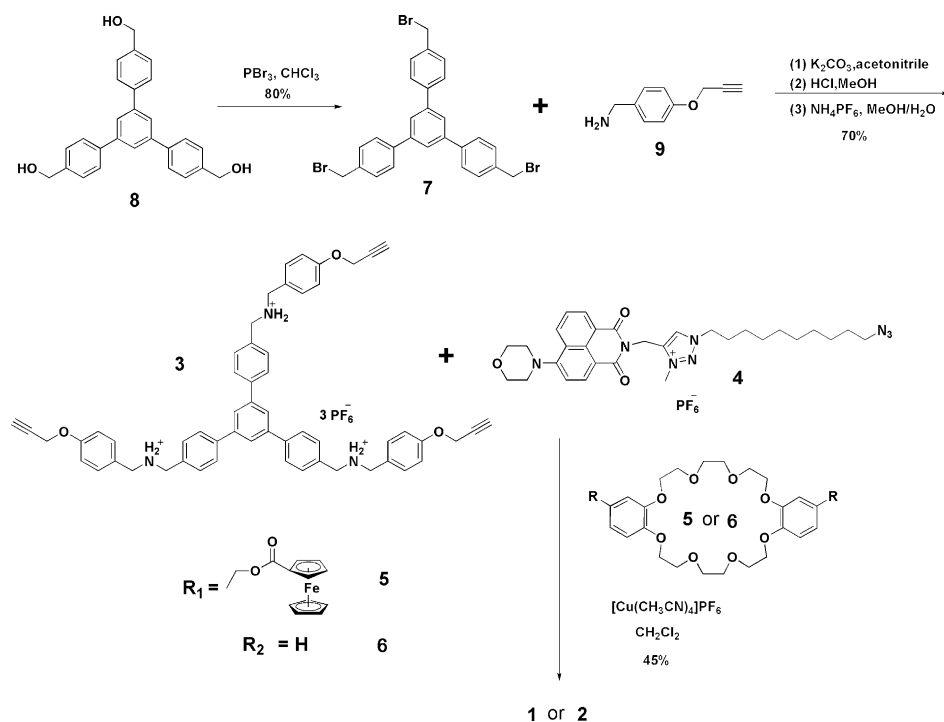
Scheme 1. Schematic representations and molecular structures of the target rotaxanes **1** and **2**.

monium (DBA)^[14] and an *N*-methyltriazolium (MTA)^[5b,7b,15] site, which are separated by a long alkyl chain, and each arm of the skeleton is terminated with a 4-morpholino-naphthalimide (MA) fluorophore^[16] as a stopper. [4]Rotaxane **1** has three di-ferrocene-functionalized DB24C8 rings threaded onto the three-armed skeleton, whereas **2** has three simple DB24C8 rings. By means of ¹H NMR spectroscopy, we have demonstrated that a reversible and uniform shuttling motion of the three macrocycles between the two recognition sites in both **1** and **2** can be driven by external acid–base stimuli, that is, the addition of 1,8-diazabicyclo[5.4.0]undec-7-ene (DBU) to deprotonate the DBA station and addition of trifluoroacetic acid (TFA) to reprotonate the secondary amine. However, [4]rotaxanes **1** and **2** show distinct modes of fluorescence modulation in response to external acid–base stimuli. In the ferrocene-functionalized [4]rotaxane **1**, the fluorescence of the MA stopper is decreased by 80% in response to the addition of DBU, which involves a tunable, distance-dependent photoinduced electron transfer (PET) process between the ferrocene (Fc) electron donors and the excited MA fluorophore. However, the fluorescence intensity of [4]rotaxane **2** shows an enhancement tendency upon addition of DBU due to the fact that the PET process between the MA fluorophore and the MTA unit is inhibited because of the encirclement of the latter by the DB24C8 ring. Both systems show good revers-

ibility. From a comparison of the different fluorescence changes, it can be concluded that the introduction of Fc units as electron donors plays an important role in the fluorescence modulation. This kind of complex topological structure has significant potential in the design and construction of large and complex topological assemblies with controllable properties and functions.

Results and Discussion

Schematic representations and the molecular structures of [4]rotaxanes **1** and **2** are shown in Scheme 1. The structural difference between the target [4]rotaxanes **1** and **2** is that **1** bears three di-ferrocene-functionalized DB24C8 rings, whereas **2** correspondingly bears three DB24C8 rings. The route for the preparation of [4]rotaxanes **1** and **2** is shown in Scheme 2. As shown in Scheme 2, the well-known noncovalent intercomponent interaction between the substituted DB24C8 ring and the DBA cation was chosen for the mechanical assembly, which has become the basis of many diverse interlocked molecular structures. Among several template-directed synthetic approaches for the construction of mechanically interlocked rotaxanes, the so-called threading-followed-by-stoppering protocol^[17] is one of the most straightforward, especially in systems with the recognition



Scheme 2. Syntheses of target [4]rotaxanes **1** and **2**.

motif provided by DB24C8/DBA, and the Cu^I-catalyzed azide–alkyne cycloaddition (CuAAC) reaction^[7b,14c,d,16b] was chosen for the stopping procedure due to its high efficiency and good functional-group tolerance. A key intermediate in the preparations of [4]rotaxanes **1** and **2** was the trifurcate compound **3**, which has a 1,3,5-triphenylene core and three arms, each of which incorporates a DBA unit as a primary recognition site for DB24C8 and a terminal alkyne as a reaction site. Starting from the known triol compound **8**, treatment with PBr₃ afforded the intermediate **7** in 80% yield. Subsequent nucleophilic substitution between tribromo-substituted compound **7** and benzylamine **9** in the presence of K₂CO₃, followed by acidification and anion exchange, afforded the key intermediate **3** in moderate yield (70%). Compound **4**, which contains a central MTA unit as a secondary recognition station, is terminated by a 4-morpholino-naphthalimide fluorescent stopper at one end and by an azide functional group at the other end. The azide **4**, the ferrocene-containing DB24C8 crown ether **5**,

8, and **9** were synthesized according to previous reports.^[2d,14b,16b,18] As shown in Scheme 2, trialkyne **3** and crown ether **5** or **6** were mixed in dry CH₂Cl₂ at room temperature, and then azide **4** and [Cu(CH₃CN)₄]PF₆ as catalyst were added. The resulting mixture was stirred for 4 days to form the target [4]rotaxane **1** or **2** in 45% isolated yield.

[4]Rotaxanes **1** and **2** were characterized by ¹H and ¹³C NMR spectroscopies and high-resolution electrospray ionization (HR-ESI) mass spectrometry. The reversible and uniform shuttling motions of the three macrocycles between the two different recognition sites in both rotaxanes **1** and **2** were also confirmed by ¹H NMR spectroscopy, as discussed below. Firstly, we analyzed the ¹H NMR spectra of

rotaxanes **1** and **2** (Figure 1). Comparison between the ¹H NMR spectra of rotaxanes **1** and **2** and our previously synthesized rotaxanes^[4c,f,5b,7b] revealed that the DB24C8 macrocycles predominately reside on the DBA recognition sites in rotaxanes **1** and **2**. The ¹H NMR spectra (Figure 1) of [4]rotaxanes **1** and **2** showed similar patterns in

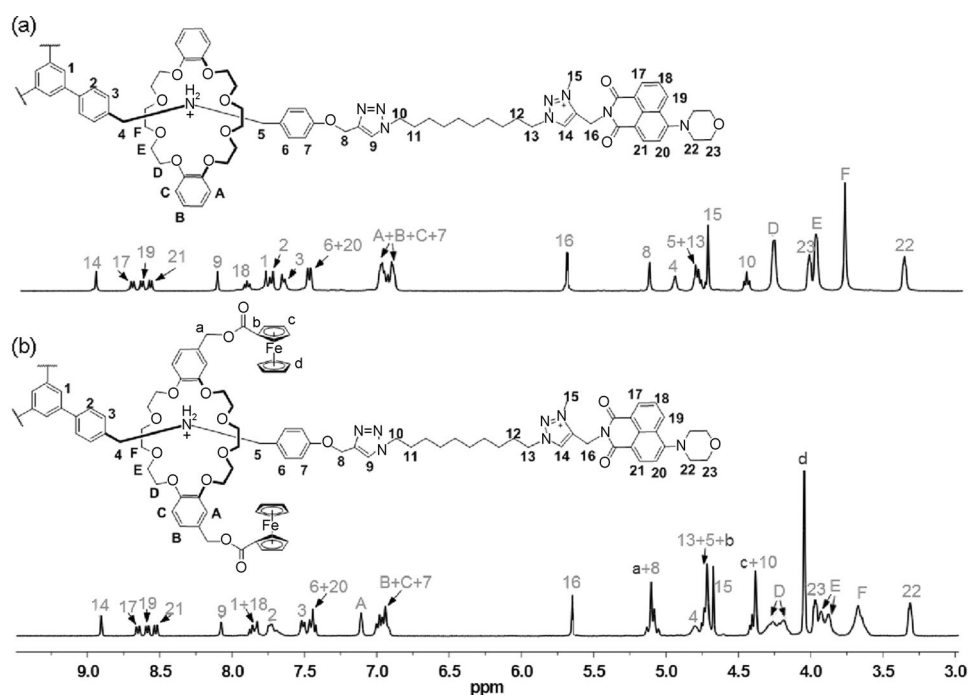


Figure 1. Partial ¹H NMR spectra (400 MHz, CD₃COCD₃, 298 K) of a) [4]rotaxane **2**, b) [4]rotaxane **1**.

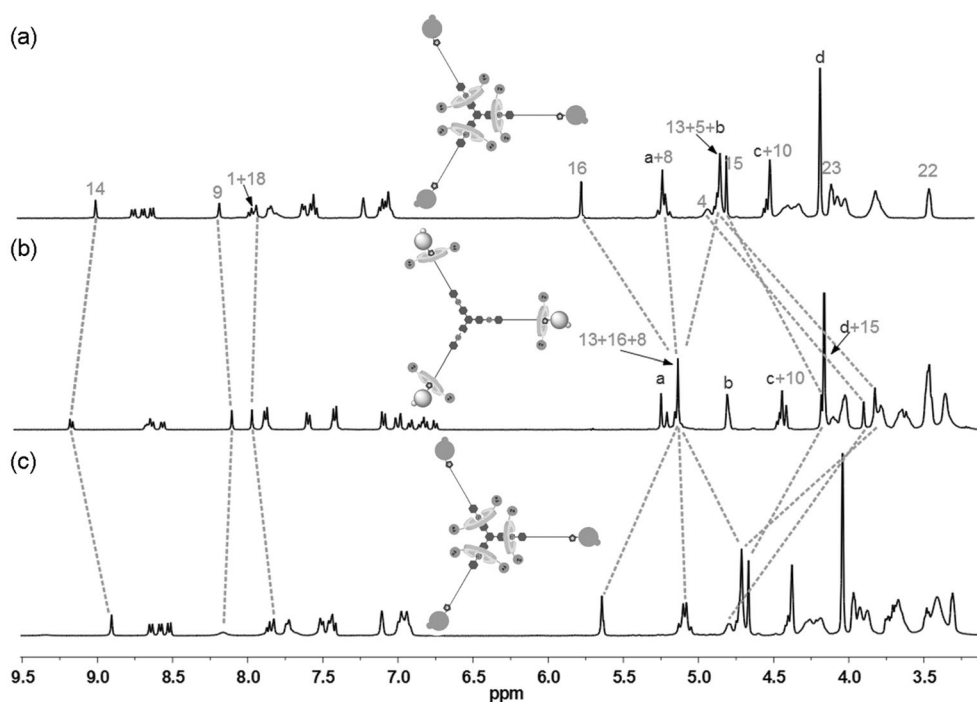


Figure 2. Partial ^1H NMR spectra (400 MHz, CD_3COCD_3 , 298 K) of a) [4]rotaxane **1**, b) the solution obtained after adding 4.0 equivalents of DBU to the solution of (a), and c) the solution obtained after adding 7.0 equivalents of CF_3COOH to the solution of (b).

CD_3COCD_3 , with no significant differences other than the absence of the peaks of H_a , H_b , H_c , and H_d of the Fc unit in the spectrum of [4]rotaxane **2**. The observed peaks could be fully assigned to the protons of **1** and **2**, as shown in Figure 1. HR-ESI mass spectra of the target [4]rotaxanes **1** and **2** also confirmed their chemical structures. The mass spectrum of [4]rotaxane **1** features major peaks at m/z 883.8276, 1089.5819, and 1398.2191, corresponding to species having lost six, five, and four PF_6^- counterions, respectively, that is, $[\text{M}-6\text{PF}_6]^6+$, $[\text{M}-5\text{PF}_6]^5+$, and $[\text{M}-4\text{PF}_6]^4+$. The HR-ESI mass spectrum of [4]rotaxane **2** features the most intense peaks at m/z 641.8239, 799.1896, and 1035.2283, again corresponding to species having lost six, five, and four PF_6^- counterions, respectively, that is $[\text{M}-6\text{PF}_6]^6+$, $[\text{M}-5\text{PF}_6]^5+$, and $[\text{M}-4\text{PF}_6]^4+$. Thus, all the experimental evidence confirmed that the target [4]rotaxanes **1** and **2** had been successfully synthesized as we had designed.

The uniform shuttling motions of the three DB24C8 macrocycles between the two distinguishable recognition stations incorporated in the three branches of [4]rotaxane **1** were confirmed by ^1H NMR spectroscopy (Figure 2). Addition of 4.0 equiv of DBU to a solution of [4]rotaxane **1** in CD_3COCD_3 resulted in deprotonation of the ammonium moieties of the DBA units to yield the free secondary amines, and as a result the macrocycle **5** migrated from the DBA station to the MTA station. As shown in Figure 2, the signals of the methylene protons H_4 and H_5 of the DBA station were significantly upfield shifted ($\Delta\delta = -0.97$ and -0.98 ppm, respectively) because of the deprotonation and the displacement of the macrocycles. The signals of the protons of the MTA station were also shifted due to association

with the macrocyclic compound **5**, with $\Delta\delta$ values of 0.34, 0.19, -0.56 , and -0.59 ppm for H_{13} , H_{14} , H_{15} , and H_{16} , respectively. All of these changes indicated that the macrocycle **5** moved to the MTA station after the addition of DBU, and thus the interactions between the DBA stations and the DB24C8 rings were lost. After reprotonation of the $-\text{NH}-$ centers by the addition of 7.0 equiv of TFA, however, the ^1H NMR spectrum was completely restored, indicating return of the DB24C8 ring to the DBA station. Thus, by ^1H NMR spectroscopic measurements, the uniform acid–base-induced reversible shuttling motion of the macrocycle along the thread component in [4]rotaxane **1** has been demonstrated.

Similarly, the shuttling motion of [4]rotaxane **2** was also confirmed by ^1H NMR spectroscopy (Figure 3). When the ammonium moiety was deprotonated by the addition of 4.0 equiv of DBU to a solution of [4]rotaxane **2** in CD_3COCD_3 , the DB24C8 macrocycle **6** migrated from the DBA recognition station to the MTA station and similar chemical shift changes as for [4]rotaxane **1** were observed. Thus, $\Delta\delta$ values of -1.07 and -0.98 ppm for H_4 and H_5 of the DBA unit and $\Delta\delta$ values of 0.34, 0.21, -0.59 , and -0.47 ppm for H_{13} , H_{14} , H_{15} , and H_{16} , respectively, of the MTA station were measured. After reprotonation of the $-\text{NH}-$ centers by the addition of 7.0 equiv of TFA, the ^1H NMR spectrum was completely restored, indicating good reversibility of the uniform acid–base-induced shuttling motions in [4]rotaxane **2**.

In these complex architectures, [4]rotaxanes **1** and **2** both have tribranched structures, each branch being a bistable [2]rotaxane arm. We also recorded the ^1H NMR spectra

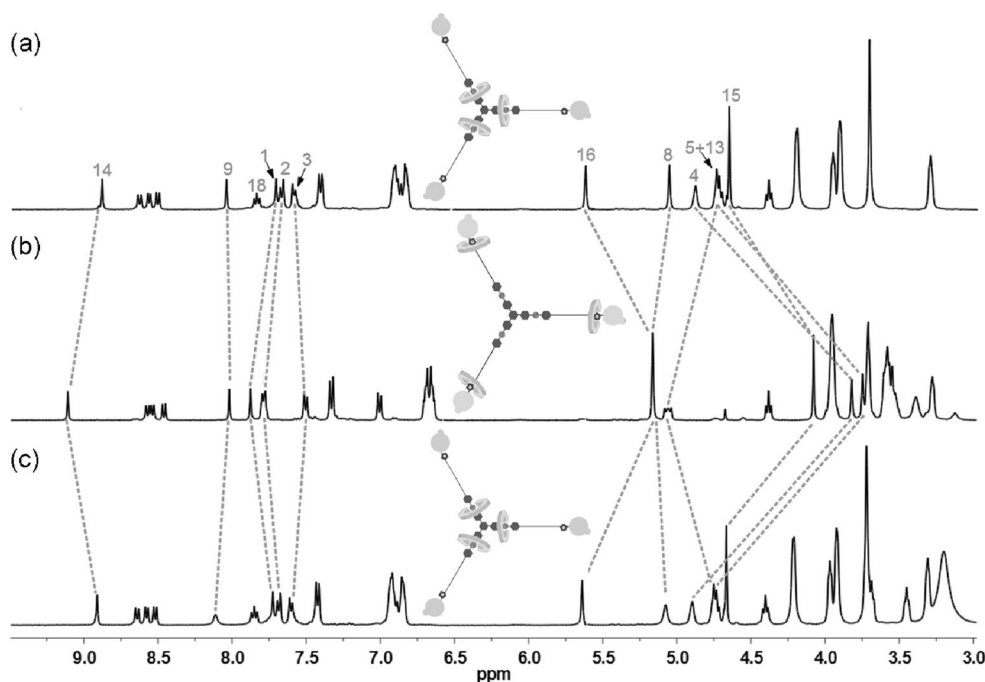


Figure 3. Partial ^1H NMR spectra (400 MHz, CD_3COCD_3 , 298 K) of a) [4]rotaxane **2**, b) the solution obtained after adding 4.0 equivalents of DBU to the solution of (a), and c) the solution obtained after adding 7.0 equivalents of CF_3COOH to the solution of (b).

(400 MHz, CD_3COCD_3 , 298 K) of [4]rotaxanes **1** and **2** upon gradual addition of DBU (Figures S14 and S15) to study the stepwise shuttling motions of the systems, that is, switching one or two of the arms selectively. Upon gradual addition of various equivalents of DBU to solutions of rotaxanes **1** and **2** in CD_3COCD_3 , the signals of the new species (macrocycle at the MTA station) gradually emerged and the signals of the original species (macrocycle at the DBA station) gradually decreased. This analysis showed that the shuttling movement of one, two, and three DB24C8 rings from the DBA to the MTA station can be driven in a stepwise manner by gradually adding DBU. Addition of excess DBU (4.0 equiv) drives all three macrocycles to the MTA station.

Next, the photophysical properties of [4]rotaxanes **1** and **2** and the reference compound **4** were determined. All three compounds exhibited an absorption band with λ_{max} at 408 nm and a strong emission band with λ_{em} at 521 nm in CH_2Cl_2 solution (Table 1 and Figure 4), typical of the MA

fluorophore. The absolute fluorescence quantum yields (Φ_f) of **1**, **2**, and **4** were measured as 11%, 55%, and 63%, respectively. It was found that [4]rotaxane **1** has the lowest fluorescence intensity of the MA moiety at 521 nm among the three compounds, and this is reasonable since there is less efficient PET from the Fc electron donors to the excited state of the MA fluorophore. This phenomenon indicates that the long alkyl chain in the structure of rotaxane **1** cannot completely inhibit the PET process, as was demonstrated in our previous reports.^[14b,16b] The time-resolved fluorescence of **1** revealed a bi-exponential decay with lifetimes of 6.6 ns (16.7%) and 1.5 ns (83.3%) (Table 1), of which the longer lifetime is the intrinsic one of the MA fluorophore, and the shorter one can be attributed to the PET process between the Fc unit and the MA fluorophore. The fluorescence spectral changes of rotaxanes **1** and **2** and compound **4** in response to the addition of DBU were also investigated (Figure 4). Upon addition of 4.0 equiv of DBU to solutions of [4]rotaxane **1** or **2** or compound **4** in CH_2Cl_2 , there were no obvious UV/Vis absorption spectral changes (Figures S1, S2, and S3), but different fluorescence change modes in the three molecular systems were observed. As shown in Figure 4a, no apparent fluorescence spectral change was observed in the solution of compound **4** after adding 4.0 equiv of DBU, which was helpful for investigating the photophysical properties of [4]rotaxanes **2** and **1**. However, different modes of fluorescence changes were observed for [4]rotaxanes **1** and **2** in response to the addition of excess DBU. Compared with the original spectrum, the emission intensity of [4]rotaxane **2** at 521 nm increased by 24% upon addition of 4.0 equiv of DBU (Figure 4b). Meanwhile, after adding

Table 1. The maximal absorption wavelength (λ_{max}), the maximal emission wavelength (λ_{em}), fluorescence lifetimes (τ), and fluorescent quantum yields (Φ_f) of **1**, **2**, and **4**.

	λ_{max} [nm]	λ_{em} [nm]	τ [ns]	Φ_f [%]
1	408	521	6.6 (16.7%), 1.5 (83.3%)	11
1 +DBU	408	521	6.8 (75.0%), 0.6 (25.0%)	1
2	408	521	6.8 (91.9%), 3.5 (8.1%)	55
2 +DBU	408	521	7.6 (91.6%), 4.0 (8.4%)	73
4	408	521	7.8 (90.1%), 4.5 (9.9%)	63
4 +DBU	408	521	7.6 (95.2%), 4.7 (4.8%)	62

[a] Rotaxanes **1** and **2** (1×10^{-5} M) and compound **4** (3×10^{-5} M) were investigated in CH_2Cl_2 at room temperature.

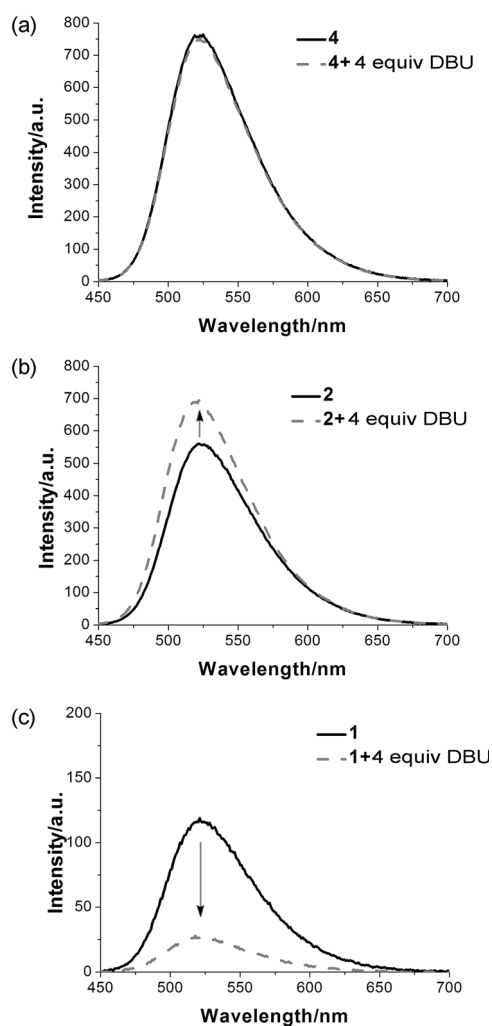


Figure 4. Fluorescence spectral changes in CH_2Cl_2 on going from rotaxanes **1** and **2** ($1 \times 10^{-5} \text{ M}$) and compound **4** ($3 \times 10^{-5} \text{ M}$) to the mixtures obtained after adding 4.0 equivalents of DBU to the solutions of **1**, **2**, and **4**. The excitation wavelength for obtaining the fluorescence spectra was 408 nm.

4.0 equiv of DBU to a solution of [4]rotaxane **2**, time-resolved fluorescence (Figures S10 and S11) showed a bi-exponential decay with lifetimes of 7.6 ns (91.6%) and 4.0 ns (8.4%) as compared to the original bi-exponential 6.8 ns (91.9%) and 3.5 ns (8.1%). This could be attributed to the movement of the DB24C8 macrocycle **6** upon addition of excess DBU. However, in the case of [4]rotaxane **1**, which has two Fc electron-donating groups on the macrocycle component, the fluorescence decreased by 80% upon addition of 4.0 equiv of DBU (Figure 4c). Time-resolved fluorescence (Figures S8 and S9) showed a bi-exponential decay with lifetimes of 6.8 ns (75.0%) and 0.6 ns (25.0%). Hence, an even shorter lifetime was observed, 0.6 ns compared with the original 1.5 ns, and the changes in fluorescence intensity and fluorescence lifetime could be ascribed to the movement of the di-ferrocene-functionalized DB24C8 rings upon addition of excess DBU. Similarly to the ^1H NMR measurements, gradual addition of DBU to solutions of [4]rotaxanes

1 and **2** in CH_2Cl_2 also resulted in gradual fluorescence spectral changes (Figures S5 and S6), again indicating that it is feasible to switch one, two, or three of the arms selectively.

By comparison of the different modes of fluorescence alteration in [4]rotaxanes **2** and **1**, we can conclude that modification of the macrocycle with Fc electron donors plays an important role in the design of such functional bistable rotaxanes. Possible mechanisms of fluorescence modulation in [4]rotaxanes **2** and **1** are depicted in Figure 5. As shown in

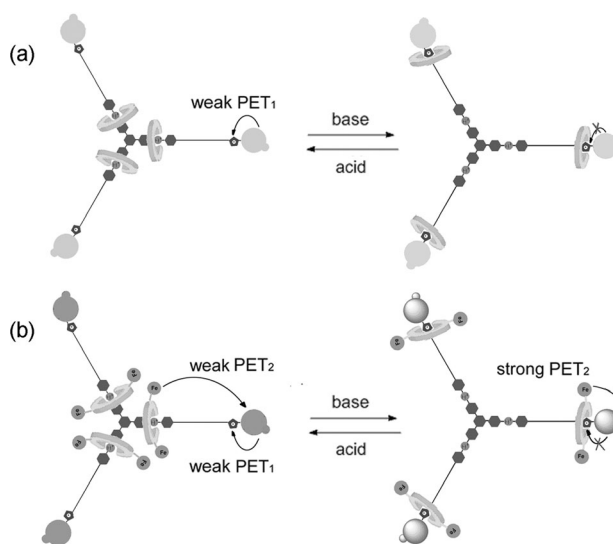


Figure 5. Schematic representations of different PET processes in a) [4]rotaxane **2** and b) [4]rotaxane **1**.

Figure 5a, there is a weak photoinduced electron transfer process (PET₁) from the MA fluorophore to the MTA moiety in the original state. After the addition of 4.0 equiv of DBU, the DB24C8 macrocycle encircles the MTA station, and as a result the PET₁ process from the MA fluorophore to the MTA station is to some extent inhibited, resulting in a modest increase in fluorescence intensity.^[4d] In contrast, upon addition of DBU to the di-ferrocene-functionalized [4]rotaxane **1**, although the PET₁ process from the MA fluorophore to the MTA station is again inhibited, resulting in a modest fluorescence increase, this effect is overwhelmed by the PET process from the electron-rich Fc unit to the electron-deficient MA fluorophore (PET₂) becoming more efficient because of the much closer proximity of the two functional groups (Figure 5b). The net effect is a remarkable fluorescence quenching.^[14b] The fluorescence change can thus be attributed to a combination of the two PET processes. The fluorescence spectra of [4]rotaxanes **1** and **2** could each be recovered upon addition of 7.0 equiv of TFA. The systems showed good reversibility and the shuttling motion of the macrocycles driven by the acid–base stimuli could be repeated many times without obvious degradation, as evidenced by reversible fluorescence change cycles of the MA fluorophore at 521 nm (Figure 6). The fluorescence cycle of compound **4** upon alternating addition

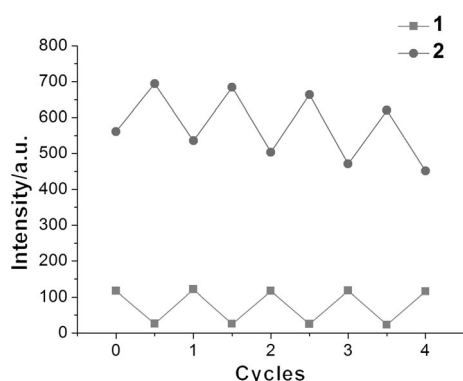


Figure 6. Fluorescence intensity changes of rotaxanes **1** and **2** (1×10^{-5} M, CH_2Cl_2) upon addition of alternate external stimuli (DBU and TFA) over four cycles. The excitation wavelength for obtaining the fluorescence spectra was 408 nm. The plotted emission intensities were recorded at 521 nm.

of DBU and TFA was also studied (Figure S7), and the fluorescence intensity exhibited a slight decrease with the number of cycles. It should be noted that the Fc-containing [4]rotaxane **1** has better reversibility than rotaxane **2** and compound **4**, which is probably due to a stabilizing effect of the Fc functional groups.

Conclusion

In summary, we have designed and constructed two novel trifurcated [4]rotaxanes **1** and **2** that have complicated branched structures with three [2]rotaxane arms that were assembled by means of CuAAC reactions. The chemical structures of the two [4]rotaxanes have been well-characterized, and the reversible and uniform shuttling motions of three DB24C8 derivative macrocycles between the DBA and MTA recognition sites in the molecular threads of [4]rotaxanes **1** and **2** have been characterized by ^1H NMR spectroscopy. Detailed investigation of the switchable photophysical properties of [4]rotaxanes **1** and **2** has indicated that a small modification by introducing ferrocene functional groups in this kind of system can lead to a different mode of function alteration, such as fluorescence modulation, which can be ascribed to the different PET processes. By comparison of the different fluorescence change modes seen for [4]rotaxanes **1** and **2**, it can be concluded that the introduction of ferrocene units as electron donors plays an important role in the fluorescence modulation. This work greatly enriches the structures and properties of the family of mechanically interlocked molecules, and this kind of symmetrical branched [n]rotaxane system with complex topological structures shows significant potential for the design and construction of large and complex assemblies with controllable properties and functions.

Experimental Section

General: ^1H and ^{13}C NMR spectra were measured on a Bruker AV-400 spectrometer. Electrospray ionization (ESI) mass spectra were acquired on an LCT Premier XE mass spectrometer. UV/Vis absorption spectra and fluorescence spectra were recorded on a Varian Cary 100 spectrometer and a Varian Cary Eclipse (1 cm quartz cells), respectively. Fluorescence lifetimes were measured by the time-correlated single-photon counting (TCSPC) technique following excitation with a nanosecond flash lamp. Fluorescence quantum yields were measured with a Fluoromax-4 fluorescence spectrophotometer equipped with a quantum yield measuring accessory and report generator program. All solvents were reagent grade and were dried and distilled prior to use according to standard procedures. Molecular structures were confirmed by ^1H and ^{13}C NMR spectroscopies and high-resolution ESI mass spectrometry. Compounds **4**, **5**, **8**, and **9** were synthesized and purified according to previous reports.^[2d,14b,16b,18]

Synthesis of compound 3: Compound **8** (0.52 g, 1.30 mmol) was dissolved in a mixture of THF (10 mL) and CHCl_3 (20 mL), the solution was cooled to 0°C , and then PBr_3 (3.52 g, 13 mmol) was slowly added. The resulting mixture was stirred for 24 h at room temperature. The reaction was then quenched with iced water (20 mL) and the mixture was extracted with CH_2Cl_2 (2×50 mL). The combined organic layers were dried over anhydrous Na_2SO_4 and concentrated to give a colorless oil. Subsequent crystallization from a mixture of methanol (50 mL) and chloroform (10 mL) afforded crystalline **7** (0.61 g, 80%) as a white solid. ^1H NMR (400 MHz, CDCl_3 , 298 K): $\delta = 7.76$ (s, 3H), 7.66 (d, $J = 8.0$ Hz, 6H), 7.52 (d, $J = 8.0$ Hz, 6H), 4.58 ppm (s, 6H). A mixture of compound **7** (0.60 g, 1.03 mmol), **9** (1.66 g, 10.3 mmol), and K_2CO_3 (0.85 g, 6.18 mmol) in acetonitrile (50 mL) was refluxed for 12 h. It was then cooled to room temperature, filtered, and the solvent was removed from the filtrate under reduced pressure. The residue was purified by column chromatography (SiO_2 ; $\text{CH}_2\text{Cl}_2/\text{MeOH}$, 100:1) to give a colorless oil. This oil was redissolved in MeOH (20 mL) and then HCl (6 M, 3 mL) was added at room temperature. After stirring for 4 h, the solvent was removed under reduced pressure. The residue was redissolved in MeOH (60 mL), and then saturated aqueous NH_4PF_6 solution (30 mL) was added. After the mixture had been stirred overnight, the MeOH was removed under vacuum, whereupon a white solid was precipitated. The crude product was collected by filtration, washed with deionized water (30 mL), and purified by column chromatography (SiO_2 ; $\text{CH}_2\text{Cl}_2/\text{MeOH}$, 50:1) to afford compound **3** (0.91 g, 70%) as a pale-yellow solid. ^1H NMR (400 MHz, CD_3COCD_3 , 298 K): $\delta = 7.98$ (s, 3H), 7.95 (d, $J = 8.0$ Hz, 6H), 7.72 (d, $J = 8.0$ Hz, 6H), 7.53 (d, $J = 8.8$ Hz, 6H), 7.07 (d, $J = 8.8$ Hz, 6H), 4.83 (d, $J = 2.0$ Hz, 6H), 4.55 (s, 6H), 4.46 (s, 6H), 3.13 ppm (t, $J = 2.0$ Hz, 3H); ^{13}C NMR (100 MHz, CD_3COCD_3 , 298 K): $\delta = 159.3$, 142.6, 142.2, 134.5, 132.3, 131.4, 130.6, 128.6, 126.2, 125.9, 117.6, 116.2, 116.1, 115.9, 79.5, 77.3, 69.4, 56.3, 52.2 ppm; HRMS: calcd for $\text{C}_{57}\text{H}_{54}\text{N}_3\text{O}_3\text{P}_2\text{F}_{12} [\text{M}-\text{PF}_6]^+$: 1118.3449; found: 1118.3439.

Synthesis of rotaxane 1: A mixture of **3** (60 mg, 0.047 mmol) and crown ether **5** (263 mg, 0.282 mmol) in dry CH_2Cl_2 (5 mL) was stirred at room temperature. Compound **4** (199 mg, 0.282 mmol) and $[\text{Cu}(\text{CH}_3\text{CN})_4]\text{PF}_6$ (52 mg, 0.14 mmol) were added to the solution, and the mixture was stirred for 4 days. After removal of the solvent, the residue was purified by column chromatography (SiO_2 ; $\text{CH}_2\text{Cl}_2/\text{MeOH}$, 50:1) to give compound **1** (131 mg, 45%) as a yellow powder. ^1H NMR (400 MHz, CD_3COCD_3 , 298 K): $\delta = 8.90$ (s, 3H), 8.65 (d, $J = 8.0$ Hz, 3H), 8.59 (d, $J = 6.8$ Hz, 3H), 8.53 (d, $J = 8.0$ Hz, 3H), 8.07 (s, 3H), 7.89–7.80 (m, 6H), 7.74 (d, $J = 8.0$ Hz, 6H), 7.51 (d, $J = 7.6$ Hz, 6H), 7.45 (d, $J = 8.0$ Hz, 6H), 7.43 (d, $J = 8.0$ Hz, 3H), 7.11 (s, 6H), 7.02–6.89 (m, 18H), 5.65 (s, 6H), 5.15–5.03 (m, 18H), 4.80 (s, 6H), 4.77–4.68 (m, 24H), 4.67 (s, 9H), 4.43–4.36 (m, 18H), 4.32–4.13 (m, 24H), 4.04 (s, 30H), 3.97 (t, $J = 7.6$ Hz, 12H), 3.95–3.81 (m, 24H), 3.73–3.59 (m, 24H), 3.31 (t, $J = 7.6$ Hz, 12H), 2.03–1.96 (m, 6H), 1.93–1.84 (m, 6H), 1.32–1.24 ppm (m, 36H); ^{13}C NMR (100 MHz, CD_3COCD_3 , 298 K): $\delta = 170.6$, 163.9, 163.3, 159.2, 156.7, 147.6, 141.2, 140.7, 140.2, 139.0, 132.9, 131.7, 131.4, 131.3, 131.2, 131.1, 129.9, 127.1, 126.1, 125.9, 124.7, 124.4, 122.6, 121.7, 115.8, 115.1, 114.8, 113.8, 113.2, 112.3, 71.4, 71.3, 70.7, 70.2, 70.0, 69.6, 68.1, 66.5, 65.3,

61.5, 54.1, 53.7, 53.4, 49.8, 38.3, 33.6, 31.9, 31.7, 30.8, 30.1, 26.1, 25.6, 22.4, 13.5 ppm; HRMS (ESI): m/z : calcd for $C_{291}H_{327}Fe_6N_{27}O_{48}$ $[M-6PF_6]^{6+}$: 883.8340; found: 883.8276; calcd for $C_{291}H_{327}Fe_6N_{27}O_{48}PF_6$ $[M-5PF_6]^{5+}$: 1089.5938; found: 1089.5819; calcd for $C_{291}H_{327}Fe_6N_{27}O_{48}P_2F_{12}$ $[M-4PF_6]^{4+}$: 1398.2334; found: 1398.2191.

Synthesis of rotaxane 2: A mixture of **3** (60 mg, 0.047 mmol) and crown ether **6** (126 mg, 0.282 mmol) in dry CH_2Cl_2 (5 mL) was stirred at room temperature. Compound **4** (199 mg, 0.282 mmol) and $[Cu(CH_3CN)_4]PF_6$ (52 mg, 0.14 mmol) were added to the solution, and the mixture was stirred for 4 days. After removal of the solvent, the residue was purified by column chromatography (SiO_2 ; $CH_2Cl_2/MeOH$, 50:1) to give compound **2** (100 mg, 45%) as a yellow powder. 1H NMR (400 MHz, CD_3COCD_3 , 298 K): δ = 8.90 (s, 3H), 8.65 (d, J = 8.0 Hz, 3H), 8.58 (d, J = 8.0 Hz, 3H), 8.52 (d, J = 8.0 Hz, 3H), 8.06 (s, 3H), 7.86 (t, J = 8.0 Hz, 3H), 7.73 (s, 3H), 7.69 (d, J = 8.4 Hz, 6H), 7.60 (d, J = 8.0 Hz, 6H), 7.43 (d, J = 8.0 Hz, 9H), 6.97–6.80 (m, 30H), 5.64 (s, 6H), 5.07 (s, 6H), 4.90 (s, 6H), 4.80–4.69 (m, 12H), 4.67 (s, 9H), 4.40 (t, J = 6.8 Hz, 6H), 4.21 (s, 24H), 3.97 (t, J = 4.0 Hz, 12H), 3.94 (s, 24H), 3.72 (s, 24H), 3.31 (t, J = 4.0 Hz, 12H), 2.04–1.95 (m, 6H), 1.94–1.83 (m, 6H), 1.31–1.24 ppm (m, 36H); ^{13}C NMR (100 MHz, CD_3COCD_3 , 298 K): δ = 163.9, 163.3, 159.1, 156.7, 147.7, 141.3, 140.9, 140.2, 132.9, 131.8, 131.4, 131.3, 131.2, 131.1, 130.0, 129.8, 127.2, 126.1, 125.9, 124.9, 124.3, 124.0, 122.6, 121.2, 115.8, 115.1, 114.7, 112.5, 70.8, 70.3, 67.8, 66.5, 61.4, 54.1, 53.7, 53.4, 52.1, 51.9, 51.8, 49.8, 38.3, 31.8, 30.9, 30.8, 30.1, 26.1, 25.6 ppm; HRMS (ESI): m/z : calcd for $C_{219}H_{267}N_{27}O_{36}$ $[M-6PF_6]^{6+}$: 641.8310; found: 641.8239; calcd for $C_{219}H_{267}N_{27}O_{36}PF_6$ $[M-5PF_6]^{5+}$: 799.1901; found: 799.1896; calcd for $C_{219}H_{267}N_{27}O_{36}P_2F_{12}$ $[M-4PF_6]^{4+}$: 1035.2289; found: 1035.2283.

Acknowledgements

We thank the Natural Science Foundation of China (21272073, 21190033) and the National Basic Research 973 Program (2011CB808400). Dr. D.-H. Qu thanks the Foundation for the Author of National Excellent Doctoral Dissertation of China (200957), the Fok Ying Tong Education Foundation (121069), the Fundamental Research Funds for the Central Universities, the Innovation Program of Shanghai Municipal Education Commission, and the Scientific Research Foundation for Returned Overseas Chinese Scholars, State Education Ministry for financial support.

- [1] a) K. Kinbara, T. Aida, *Chem. Rev.* **2005**, *105*, 1377–1400; b) W. R. Browne, B. L. Feringa, *Nat. Nanotechnol.* **2006**, *1*, 25–35; c) H. Tian, Q.-C. Wang, *Chem. Soc. Rev.* **2006**, *35*, 361–374; d) E. R. Kay, D. A. Leigh, F. Zerbetto, *Angew. Chem.* **2007**, *119*, 72–196; *Angew. Chem. Int. Ed.* **2007**, *46*, 72–191; e) S. Saha, J. F. Stoddart, *Chem. Soc. Rev.* **2007**, *36*, 77–92; f) B. Champin, P. Mobian, J.-P. Sauvage, *Chem. Soc. Rev.* **2007**, *36*, 358–366; g) V. Balzani, A. Credi, M. Venturi, in *Molecular Devices and Machines – Concepts and Perspectives for the Nanoworld*, Wiley-VCH, Weinheim, **2008**; h) R. J. Puddephatt, *Chem. Soc. Rev.* **2008**, *37*, 2012–2027; i) K. M. Mullen, P. D. Beer, *Chem. Soc. Rev.* **2009**, *38*, 1701–1713; j) V. Balzani, A. Credi, M. Venturi, *Chem. Soc. Rev.* **2009**, *38*, 1542–1550; k) D.-H. Qu, H. Tian, *Chem. Sci.* **2011**, *2*, 1011–1015; l) V. Balzani, A. Credi, M. Venturi, in *Molecular Devices and Machines – A Journey into the Nano World*, Wiley-VCH, Weinheim, **2003**; D.-H. Qu, H. Tian, *Chem. Sci.* **2013**, *4*, 3031–3035.
- [2] a) Z. J. O'Brien, S. D. Karlen, S. Khan, M. A. Garcia-Garibay, *J. Org. Chem.* **2010**, *75*, 2482–2491; b) X. Ma, H. Tian, *Chem. Soc. Rev.* **2010**, *39*, 70–80; c) L. Kobr, K. Zhao, Y.-Q. Shen, A. Comotti, S. Bracco, R. K. Shoemaker, P. Sozzani, N. A. Clark, J. C. Price, C. T. Rogers, J. Michl, *J. Am. Chem. Soc.* **2012**, *134*, 10122–10131; d) A. Arduini, R. Bussolati, A. Credi, S. Monaco, A. Secchi, S. Silvi, M. Venturi, *Chem. Eur. J.* **2012**, *18*, 16203–16213; e) A.-M. L. Fuller, D. A. Leigh, P. J. Lusby, *J. Am. Chem. Soc.* **2010**, *132*, 4954–4959; f) P.-N. Cheng, P.-Y. Huang, W.-S. Li, S.-H. Ueng, W.-C. Hung, Y.-H. Liu, C.-C. Lai, Y. Wang, S.-M. Peng, I. Chao, S.-H. Chiu, *J. Org. Chem.* **2006**, *71*, 2373–2383; g) L.-L. Zhu, H. Yan, K. T. Nguyen, H. Tian, Y.-L. Zhao, *Chem. Commun.* **2012**, *48*, 4290–4292.
- [3] a) J. D. Crowley, D. A. Leigh, P. J. Lusby, R. T. McBurney, L. E. Perret-Aebi, C. Petzold, A. M. Z. Slawin, M. D. Symes, *J. Am. Chem. Soc.* **2007**, *129*, 15085–15090; b) S. Saha, A. H. Flood, J. F. Stoddart, S. Impellizzeri, S. Silvi, M. Venturi, A. Credi, *J. Am. Chem. Soc.* **2007**, *129*, 12159–12171; c) G. Fioravanti, N. Haraszkiwicz, E. G. Kay, S. M. Mendoza, C. Bruno, M. Marcaccio, P. G. Wiering, F. Paolucci, P. Rudolf, A. M. Brouwer, D. A. Leigh, *J. Am. Chem. Soc.* **2008**, *130*, 2593–2601; d) A. Coskun, D. C. Friedman, H. Li, K. Patel, H. A. Khatib, J. F. Stoddart, *J. Am. Chem. Soc.* **2009**, *131*, 2493–2495; e) A. Mateo-Alonso, *Chem. Commun.* **2010**, *46*, 9089–9099; f) S. Dasgupta, J.-S. Wu, *Chem. Sci.* **2012**, *3*, 425–432; g) A. Mateo-Alonso, D. M. Guldi, F. Paolucci, M. Prato, *Angew. Chem.* **2007**, *119*, 8266–8272; *Angew. Chem. Int. Ed.* **2007**, *46*, 8120–8126.
- [4] a) D.-H. Qu, Q.-C. Wang, H. Tian, *Angew. Chem.* **2005**, *117*, 5430–5433; *Angew. Chem. Int. Ed.* **2005**, *44*, 5296–5299; b) Q.-C. Wang, X. Ma, D.-H. Qu, H. Tian, *Chem. Eur. J.* **2006**, *12*, 1088–1096; c) H. Zhang, X.-X. Kou, Q. Zhang, D.-H. Qu, H. Tian, *Org. Biomol. Chem.* **2011**, *9*, 4051–4056; d) W.-L. Yang, Y.-J. Li, Y. Zhang, W. Yu, T.-F. Liu, H.-B. Liu, Y.-L. Li, *Org. Biomol. Chem.* **2011**, *9*, 6022–6026; e) T. Ogoishi, D. Yamafuji, T. Aoki, T.-a. Yamagishi, *Chem. Commun.* **2012**, *48*, 6842–6844; f) H. Zhang, B. Zhou, H. Li, D.-H. Qu, H. Tian, *J. Org. Chem.* **2013**, *78*, 2091–2098; g) C.-J. Zhang, S.-J. Li, J.-Q. Zhang, K. L. Zhu, N. Li, F.-H. Huang, *Org. Lett.* **2007**, *9*, 5553–5556; h) S.-Y. Dong, X.-Z. Yan, B. Zheng, J.-Z. Chen, X. Ding, Y.-H. Yu, D.-H. Xu, M.-M. Zhang, F.-H. Huang, *Chem. Eur. J.* **2012**, *18*, 4195–4199; i) A. Mateo-Alonso, P. Brough, M. Prato, *Chem. Commun.* **2007**, 1412–1414; j) A. Mateo-Alonso, G. Fioravanti, M. Marcaccio, F. Paolucci, G. M. A. Rahman, C. Ehli, D. M. Guldi, M. Prato, *Chem. Commun.* **2007**, 1945–1947.
- [5] a) Z.-J. Zhang, H.-Y. Zhang, H. Wang, Y. Liu, *Angew. Chem.* **2011**, *123*, 11026–11030; *Angew. Chem. Int. Ed.* **2011**, *50*, 10834–10838; b) H. Zhang, Q. Liu, J. Li, D.-H. Qu, *Org. Lett.* **2013**, *15*, 338–341; c) J.-M. Han, Y.-H. Zhang, X.-Y. Wang, C.-J. Liu, J.-Y. Wang, J. Pei, *Chem. Eur. J.* **2013**, *19*, 1502–1510.
- [6] a) J. D. Badjić, V. Balzani, A. Credi, J. N. Lowe, S. Silvi, J. F. Stoddart, *Chem. Eur. J.* **2004**, *10*, 1926–1935; b) J. D. Badjić, C. M. Ronconi, J. F. Stoddart, V. Balzani, S. Silvi, A. Credi, *J. Am. Chem. Soc.* **2006**, *128*, 1489–1499.
- [7] a) D. Zhang, Q. Zhang, J.-H. Su, H. Tian, *Chem. Commun.* **2009**, 1700–1702; b) H. Li, H. Zhang, Q. Zhang, Q.-W. Zhang, D.-H. Qu, *Org. Lett.* **2012**, *14*, 5900–5903; c) D.-H. Qu, F.-Y. Ji, Q.-C. Wang, H. Tian, *Adv. Mater.* **2006**, *18*, 2035–2038; d) H. Tian, *Angew. Chem.* **2010**, *122*, 4818–4820; *Angew. Chem. Int. Ed.* **2010**, *49*, 4710–4712.
- [8] a) E. Ishow, A. Credi, V. Balzani, F. Spadola, L. Mandolini, *Chem. Eur. J.* **1999**, *5*, 984–989; b) W. Zhou, J. Li, X. He, C. Li, J. Lv, Y. Li, S. Wang, H. Liu, D. Zhu, *Chem. Eur. J.* **2008**, *14*, 754–763; c) W. Zhou, S. Zhang, G. Li, Y. Zhao, Z. Shi, H. Liu, Y. Li, *ChemPhysChem* **2009**, *10*, 2066–2072; d) A. Mateo-Alonso, C. Ehli, D. M. Guldi, M. Prato, *J. Am. Chem. Soc.* **2008**, *130*, 14938–14939; e) A. Mateo-Alonso, C. Ehli, G. M. A. Rahman, D. M. Guldi, G. Fioravanti, M. Marcaccio, F. Paolucci, M. Prato, *Angew. Chem.* **2007**, *119*, 3591–3595; *Angew. Chem. Int. Ed.* **2007**, *46*, 3521–3525; f) A. Mateo-Alonso, M. Prato, *Eur. J. Org. Chem.* **2010**, 1324–1332.
- [9] a) H. Onagi, J. J. Rebek, *Chem. Commun.* **2005**, 4604–4606; b) Y. Li, H. Li, Y. Li, H. Liu, S. Wang, X. He, N. Wang, D. Zhu, *Org. Lett.* **2005**, *7*, 4835–4838; c) X.-Y. Wang, J.-M. Han, J. Pei, *Chem. Asian J.* **2012**, *7*, 2429–2437.
- [10] a) Q. Jiang, H.-Y. Zhang, M. Han, Z.-J. Ding, Y. Liu, *Org. Lett.* **2010**, *12*, 1728–1731; b) J. Yin, C. Chi, J. Wu, *Org. Biomol. Chem.* **2010**, *8*, 2594–2599; c) Z.-J. Zhang, Y.-M. Zhang, Y. Liu, *J. Org. Chem.* **2011**, *76*, 4682–4685; d) A. Mateo-Alonso, K. Iliopoulos, S. Couris, M. Prato, *J. Am. Chem. Soc.* **2008**, *130*, 1534–1535.
- [11] a) D.-H. Qu, Q.-C. Wang, J. Ren, H. Tian, *Org. Lett.* **2004**, *6*, 2085–2088; b) E. M. Pérez, D. T. F. Dryden, D. A. Leigh, G. Teobaldi, F. Zerbetto, *J. Am. Chem. Soc.* **2004**, *126*, 12210–12211; c) X. Ma, D.-

- H. Qu, F.-Y. Ji, Q.-C. Wang, L.-L. Zhu, Y. Xu, H. Tian, *Chem. Commun.* **2007**, 1409–1411.
- [12] a) H. V. Ly, J. Moilanen, H. M. Tuononen, M. Parvez, R. Roesler, *Chem. Commun.* **2011**, 47, 8391–8393; b) F. Scarel, G. Valenti, S. Gakwad, M. Marcaccio, F. Paolucci, A. Mateo-Alonso, *Chem. Eur. J.* **2012**, 18, 14063–14073; c) A. H. Flood, J. F. Stoddart, D. W. Steuerman, J. R. Heath, *Science* **2004**, 306, 2055–2056.
- [13] a) C. Gao, S. Silvi, X. Ma, H. Tian, M. Venturi, A. Credi, *Chem. Commun.* **2012**, 48, 7577–7579; b) G. Bottari, D. A. Leigh, E. M. Pérez, *J. Am. Chem. Soc.* **2003**, 125, 13360–13361.
- [14] a) Y. Jiang, J.-B. Guo, C.-F. Chen, *Org. Lett.* **2010**, 12, 4248–4251; b) H. Zhang, J. Hu, D.-H. Qu, *Org. Lett.* **2012**, 14, 2334–2337; c) C. Clavel, C. Romuald, E. Brabet, F. Coutrot, *Chem. Eur. J.* **2013**, 19, 2913; d) W. Zhou, Y.-J. Guo, D.-H. Qu, *J. Org. Chem.* **2013**, 78, 590–596; e) M. Baroncini, S. Silvi, M. Venturi, A. Credi, *Angew. Chem.* **2012**, 124, 4299–4302; *Angew. Chem. Int. Ed.* **2012**, 51, 4223–4226; f) F. Wang, C. Han, C. He, Q. Zhou, J. Zhang, C. Wang, N. Li, F. Huang, *J. Am. Chem. Soc.* **2008**, 130, 11254–11255.
- [15] a) W. Zhou, H. Zhang, H. Li, Y. Zhang, Q.-C. Wang, D.-H. Qu, *Tetrahedron* **2013**, 69, 5319–5325; b) Z.-J. Zhang, M. Han, H.-Y. Zhang, Y. Liu, *Org. Lett.* **2013**, 15, 1698–1701; c) D.-H. Qu, B. L. Feringa, *Angew. Chem.* **2010**, 122, 1125–1128; *Angew. Chem. Int. Ed.* **2010**, 49, 1107–1110; d) D. Tu, L. Liu, Q. Ju, Y. Liu, H. Zhu, R. Li, X. Chen, *Angew. Chem.* **2011**, 123, 6430–6434; *Angew. Chem. Int. Ed.* **2011**, 50, 6306–6310.
- [16] a) A. Mateo-Alonso, C. Ehli, D. M. Guldi, M. Prato, *Org. Lett.* **2013**, 15, 84–87; b) H. Li, J.-N. Zhang, W. Zhou, H. Zhang, Q. Zhang, D.-H. Qu, H. Tian, *Org. Lett.* **2013**, 15, 3070–3073.
- [17] a) T. Ogoshi, R. Shiga, T.-a. Yamagishi, *J. Am. Chem. Soc.* **2012**, 134, 4577–4580; b) G. T. Spence, M. B. Pitak, P. D. Beer, *Chem. Eur. J.* **2012**, 18, 7100–7108; c) T. Ogoshi, K. Demachi, K. Masaki, T.-a. Yamagishi, *Chem. Commun.* **2013**, 49, 3952–3954.
- [18] J. Brunel, I. Ledoux, J. Zyss, M. Blanchard-Desce, *Chem. Commun.* **2001**, 923–924.

Received: July 31, 2013

Revised: September 5, 2013

Published online: November 7, 2013